DIFFUSE REFLECTANCE SPECTROSCOPY OF IRON OXIDES

José Torrent
Vidal Barrón
Universidad de Córdoba, Córdoba, Spain

INTRODUCTION

Color is one of the most conspicuous attributes of iron oxides, oxihydroxides, and hydroxides, which are collectively referred to as Fe oxides in this article. This attribute has been the basis for many uses of Fe oxides, the earliest of which was as pigments in prehistoric paintings. The variety of colors exhibited by the Fe oxides result from different types of electronic transitions. As a rule, colored Fe oxides adsorb strongly in the ultraviolet (UV) and blue spectral regions but are strongly reflecting in the red and infrared (IR) regions. There are marked differences in this respect among individual oxides, however. In fact, any ''warm'' hue, from yellow in goethite (α-FeOOH) to purple red in some hematites (α-Fe_2O_3), can be observed. As shown later in this article, these differences are the basis for distinction to some extent among Fe oxides (1).

In nature, and in some industrial products, Fe oxides occur generally as small particles, either in pure form or intimately mixed with particles of other minerals or diluents. When a beam of incident light impinges on the surface of these powdered materials, only a small fraction is specularly reflected, the remainder penetrating into the mass and undergoing scattering (viz. multiple reflections, refractions, and diffraction in all directions) and wavelength-dependent absorption within the colored material. Part of this radiation ultimately leaves the mass in all directions and constitutes so-called *diffusely reflected light* (2, 3). The analysis of corresponding diffuse reflectance (DR) spectra has proved useful to identify and characterize different types of Fe oxides. As a result, the DR techniques have gained acceptance for this purpose since the 1980s (4, 5). However, the full potential of these techniques has not yet been fully explored. In this article, we examine the basic principles and assumptions of the DR spectroscopy, the obtention and parametrization of DR spectra in the visible and IR regions, and finally, their use in the identification and characterization of Fe oxides.

ACQUISITION OF DIFFUSE REFLECTANCE SPECTRA

DR spectra are usually obtained by using a spectrophotometer equipped with a DR accesory capable of collecting the reflected flux. This accesory has an internal surface, with a spherical (''integrating sphere'') or any other suitable geometry that is coated with a white standard intended to collect the light reflected by standard and sample. Modern double-beam spectrophotometers are equipped with holders where the powdered sample and the white standard are tightly packed. The standard is usually $BaSO_4$, MgO, or polytetrafluoroethylene (PTFE) and exhibit near-unity reflectance in the wavelength range of interest (from the near UV to the near IR).

There is no standard method of sample preparation in DR spectroscopy. Usually, finely ground powder of a standard or sample is carefully packed into a sample holder with a rectangular or circular hole with a surface of a few tens square millimeters to several square centimeters. No special care need be exercised when the holder is placed horizontally at the bottom of the integrating sphere, but self-supporting powder mounts are required when the holder is placed vertically. It is advisable in the latter case to strongly press the powder against unglazed white paper to prevent it from falling into the integrating sphere and avoid undesired particle orientations. Unfortunately, even with unglazed paper, particle orientation can occur, particularly in samples consisting of Fe oxide particles of certain sizes and shapes (e.g., fine-grained specular hematite). Grinding of the sample can cause dramatic changes in color and in some features of the DR spectrum (4, 6). A need thus exists to standardize the grinding procedure, whether mechanical (e.g., with a ball mill) or by use of the conventional agate mortar and pestle. Also, when samples are diluted with a white standard or an appropriate diluent (either to prevent orientation or because the sample is scant), a fixed dilution factor must be used in comparing samples.

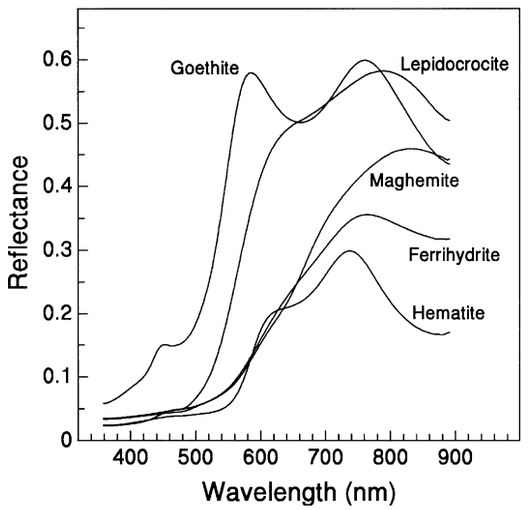

Fig. 1 Diffuse reflectance spectra for various fine-size (<500 nm) synthetic Fe oxides.

Data acquisition and processing in modern spectrophotometers are performed by built-in microprocessors or standalone computers. A spectrum from the near UV to the near IR range in 0.5- or 1-nm steps is usually obtained within a few minutes and can be stored in a convenient file format for subsequent use.

Fig. 1 shows the DR spectra for various Fe oxides. The spectra, which were recorded at 0.5-nm intervals, are smooth curves the ordinate (reflectance) of which increases as the light goes from blue (~450 nm) to red (~650 nm).

COLOR NOTATION AND CALCULATIONS

A diffuse reflectance spectrum can be converted into a color by using the basic concepts underlying the perception of this attribute by the human eye. In essence, any radiant flux that impinges on the eye (an *external stimulus*) is perceived as an *internal stimulus* (7). Psychophysically, any color can be identified by only three color stimuli, a *color stimulus* being radiant energy of a given intensity and spectral composition entering the eye and producing a sensation of color (7). Therefore, any spectrum reaching a standard observer's eye can be converted into the so-called *tristimulus values*, conveniently designated as X, Y, and Z (7). Obviously, the tristimulus values (i.e., the ''color'') of an object depend both on the intrinsic reflecting properties of the object and on the type of illuminating light. As a result, converting the DR spectrum provided by a spectrophotometer into X, Y, and Z values entails adopting a standard illuminant.

The X, Y, and Z values are usually converted into the *chromaticity coordinates* $x = X/(X+Y+Z)$ and $y = Y/(X+Y+Z)$. These coordinates, together with the Y value, define a region of well-defined limits in a 3-D space that is called *a color solid*. This solid comprises all the colors achievable under a certain illuminant. Unfortunately, the Euclidean distances in this xyY space are poorly correlated with visual differences. For this reason, color scientists generated more ''uniform'' color spaces, which are those currently used in science and industry. Many Earth scientists use the Munsell Color System, which is based on cylindrical coordinates for the variables *hue* (the attribute of a color percepetion denoted by blue, yellow, red, and so on), *value* (the lightness of a color), and *chroma* (the degree to which a stimulus differs from an achromatic, i.e., gray, stimulus). The Munsell Books of Color (available through Munsell Color, New Windsor, NY) present color chips arranged on constant-hue charts. In the charts of interest for the Fe oxides, hue changes from yellow to red to red-purple in the sequence 5Y → 2.5Y → 10YR → 7.5YR → ... → 2.5YR → 10R → 7.5R...→ 5RP. On each chart, value increases with the ordinate and chroma with the abscissa (Fig. 2).

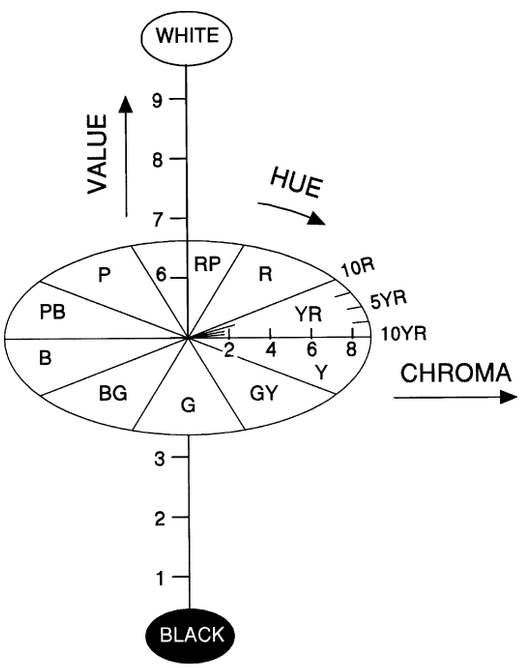

Fig. 2 Arrangement of cylindrical coordinates hue, value, and chroma in the Munsell color space. (From Ref. 4.)

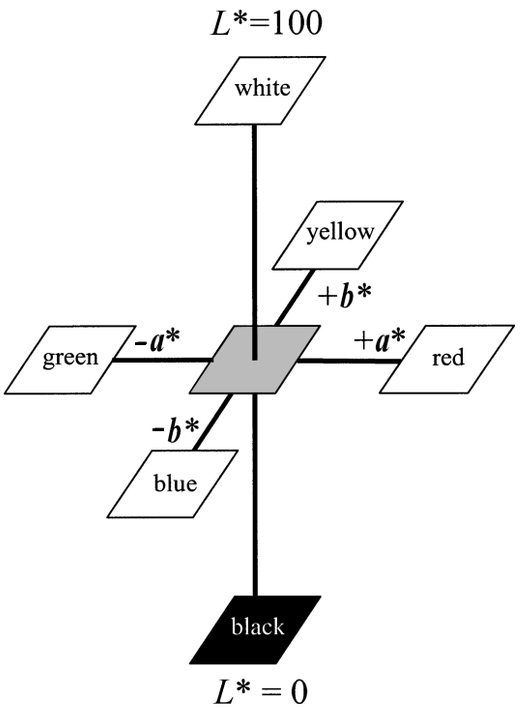

Fig. 3 Arrangement of color attributes in the CIE 1976 ($L^*a^*b^*$) color space.

The most frequently used modern system is the CIE 1976 ($L^*a^*b^*$) space (8), which provides an effective means for visualizing color: the L^*-axis represents ''lightness-darkness'', the a^*-axis ''redness-greenness'', and the b^*-axis ''yellowness-blueness'' (Fig. 3). Unfortunately, this system is not widely used among Earth scientists.

Color in the Munsell, CIE 1976 ($L^*a^*b^*$) and some other systems can also be measured with photoelectric tristimulus colorimeters, which possess a source–filter–photodetector combination that allows measurement of the approximate X, Y, and Z values of an object (but not of the DR spectrum). Colorimeters are easy and fast to operate, and usually allow viewing of large sample areas. However, they are inadequately accurate for some purposes and possess one or two built-in illuminants at most.

COLOR OF IRON OXIDES

Each individual Fe oxide exhibits a color that is mainly a function of the electron transitions allowed by its structure. Other factors significantly affecting color include particle size and shape, crystal defects, adsorbed impurities, and the degree of particle packing.

Particle size is a primary source of color differences among specimens of the same material (2). Such differences can be dramatic in iron oxides; thus, specular hematite (specularite) is black but turns bright red when ground to micron size. Generally, a reduction in particle size of Fe oxides results in paler colors; one exception is goethite (9, 10). Unfortunately, it is difficult to rationalize the particle-size effect on the lightness and, particularly, hue of the Fe oxides, and the same applies to the influence of shape.

Aggregation and cementation of individual particles are known to influence the color of many natural Fe oxides in a way generally similar to that of an increase in particle size. Thus, Torrent and Schwertmann (6) observed that sediments containing hematites that differed little in particle size ranged widely in hue (from yellowish-red to purple). However, the hues of the sediments became similar (yellowish-red) upon gentle grinding. The authors hypothesized that the purple sediments contained particles of yellowish-red hematite in aggregates that behaved optically as large (purple) hematite particles. Upon disruption of the aggregates by grinding, the color of the sediment was dictated by that of the individual hematite particles.

The color of most Fe oxides is highly sensitive to crystal impurities and defects. Thus, Al-for-Fe substitution results in an increase in hematite lightness (11) and chroma (12), and also in the redness of goethite (12). Goethites prepared with structural V possess olive hues (unpublished data); on the other hand, incorporation of structural Mn results in a marked decrease in goethite lightness (13).

Scheinost and Schwertmann (1) examined the color of 277 synthetic and natural fine-size, single-mineral samples of seven Fe oxides and two hydroxysulfates (goethite, hematite, lepidocrocite, maghemite, ferrihydrite, akaganéite, feroxyhyte, schwertmannite, and jarosite). Magnetite (black) and wüstite (a ferrous oxide) were excluded from this study, some of which results are shown in Table 1. Munsell hue ranged from ~4Y (yellow) to ~4R (red), value from ~2.5 to ~8, and chroma from ~1.5 to ~9. Similarly, CIE-xyY and CIE 1976 ($L^*a^*b^*$) coordinates varied over wide ranges.

As can be seen from Table 1, there was no overlap between the (red) hue of hematite and the (yellow) hue of goethite. The jarosites were always yellower than the goethites and the remaining oxides filled the gap between the average hue of hematite and that of goethite, thus making distinction solely by hue impossible. The same authors used discriminant analysis and found that the best separation between minerals was achieved in the CIE-xyY, followed by the CIE 1976 ($L^*a^*b^*$) space and the Munsell system (79%, 77%, and 75% of all samples correctly

Table 1 Colors of synthetic and natural Fe oxides and hydroxysulfates

Fe oxide	Formula	Most frequent color	No. of samples	Origin	Munsell color (median and range)		
					Hue	Value	Chroma
Goethite	α-FeOOH	Brownish-yellow	82	S	0.4Y (7.3YR–1.6Y)	6.0 (4.0–6.8)	6.9 (6.0–7.9)
Hematite	α-Fe_2O_3	Red	59	S	1.2YR (3.5R–4.1YR)	3.6 (2.4–4.4)	5.2 (1.5–7.9)
Lepidocrocite	γ-FeOOH	Reddish-yellow	32	S	6.8YR (4.9–7.9)	5.5 (4.6–5.9)	8.2 (7.1–9.9)
Maghemite	γ-Fe_2O_3	Dark brown	7	S	8.3YR (6.2YR–9.4)	3.1 (2.5–3.6)	3.2 (2.5–4.1)
Ferrihydrite	$Fe_5HO_8{\cdot}4H_2O$	Strong brown	59	NS	6.6YR (2.8YR–9.2YR)	4.9 (2.3–6.3)	6.3 (1.9–7.3)
Feroxyhyte	δ-FeOOH	Yellowish-red	10	NS	4.2YR (3.7YR–5.4YR)	3.8 (3.4–4.7)	6.0 (5.5–7.0)
Akaganéite	β-FeOOH	Yellowish-red	8	S	5.2YR (1.2YR–6.8YR)	3.8 (2.8–4.3)	5.8 (4.4–7.3)
Schwertmannite	$Fe_8O_8(OH)_6SO_4$	Reddish-yellow	16	NS	8.5YR (6.2YR–0.3Y)	5.9 (4.7–6.7)	6.9 (4.0–9.1)
Jarosite	$MFe_3(OH)_6(SO_4)_2$	Yellow	4	N	3.0Y (2.6Y–3.6Y)	7.8 (7.4–8.0)	5.1 (3.8–6.2)

S = synthetic; N = natural.
(From Ref. 1.)

classified, respectively). This suggests that the choice of the color system is relatively unimportant. The identification of ferrihydrites, akaganéites, and schwertmannites largely failed because of similar colors and high color variability. However, goethite, hematite, lepidocrocite, jarosite, maghemite, and feroxyhyte could be identified with relatively high reliability.

Indices obtained by mathematical combination of coordinates of different color spaces are sometimes used to quantify Fe oxides in mixtures. For instance, a ''redness rating'' (RR) based on the Munsell notation and proposed by Torrent et al. (14) proved useful to quantify hematite in mineral mixtures and soils (15–19). These indices, however, provide no better results than the use of color coordinates to discriminate among Fe oxides. For this purpose, rigurous interpretation of the DR spectra for Fe oxides is usually a better alternative as shown below.

DIFFUSE REFLECTANCE SPECTRA OF IRON OXIDES

Parameterization Procedures and Applications: The Kubelka–Munk Theory

Visual inspection of the raw spectra of Fe oxides (Fig. 1) provides little information on the optical properties of these compounds. In practice, any spectrum must be parameterized to make the information contained in it useful. One immediate parameterization procedure involves calculating the tristimulus values and color coordinates as discussed before. Other parameterization procedures involve mathematical transformations of the DR data and comparisons of the transformed data for different wavelengths. The most useful transformation of reflectance data is provided by the theory of Kubelka–Munk (20), which holds when the dimensions of the particles are comparable with, or smaller than, the wavelength of the incident light, and the diffuse reflection no longer allows one to separate the contribution of the reflection, refraction, and diffraction (i.e., scattering occurs). The basic differential equations of this theory assume that, when a layer of thickness du of a mixture of small particles is irradiated in a direction normal to its surface, the downward diffuse flux, i, is decreased by absorption by $Kidu$ and also decreased by an amount $Sidu$ by scattering. In turn, the upward flux, j, is increased by $Sidu$ and decreased by $Kjdu$. The K and S values are called the *absorption* and *scattering* coefficients of the pigment mixture layer. In the explicit hyperbolic solution of these differential equations, the reflectance, R, is expressed as a function of the reflectance of the background beneath the layer, the thickness of the layer and K and S (21). In the

limiting case of an infinitely thick sample (which for most mixtures containing Fe oxides occurs for a few tenths of a millimeter), thickness has no influence on the value of R. In this case, the Kubelka–Munk equation at any wavelength becomes

$$\frac{K}{S} = \frac{(1-R_\infty)^2}{2R_\infty} \equiv F(R_\infty) \quad (1)$$

where R_∞ is the limiting reflectance, and the $F(R_\infty)$ is the so-called *remission* or *Kubelka–Munk* function.

Duncan (22) showed that the absorption and scattering coefficients of a mixture of pigments (K_m, S_m) can be treated as a linear combination of the respective coefficients of the pigments in the mixture weighted according to the proportion of each pigment:

$$K_m = C_1K_1 + C_2K_2 + \ldots C_nK_n \quad (2)$$

$$S_m = C_1S_1 + C_2S_2 + \ldots C_nS_n \quad (3)$$

where C is the proportion (in mass) of a pigment and subscripts 1, 2, $\ldots n$ refer to the different pigments in the mixture.

Eqs. 2 and 3 are the basis for estimating the proportions of the different pigments in a mixture provided K and S for each pigment are known. The values of the unknowns (C_1, $C_2, \ldots C_n$) can then be obtained by using these equations at n different wavelengths. In practice, it is useful to use more wavelengths and apply a least-square minimization procedure to estimate the C values.

K and S for a pigment can be determined by mixing it with a white standard in variable proportions. Eqs. 2 and 3 thus become

$$K_m = C_pK_p + C_sK_s \quad (4)$$

$$S_m = C_pS_p + C_sS_s \quad (5)$$

where subscripts p and s denote pigment and white standard, respectively.

By combining Eq. 1 with Eqs. 4 and 5, we obtain

$$\frac{K_M}{S_M} = \frac{(1-R_M)^2}{2R_M} = \frac{C_pK_p + C_sK_s}{C_pS_p + C_sS_s} \quad (6)$$

If we assign a unity reflectance to the white standard, K_s is zero according to Eq. 1. Eq. 6 can then be expressed as

$$\frac{2R_M}{(1-R_M)^2} = \frac{C_pS_p + C_sS_s}{C_pK_p} = \frac{S_p}{K_p} + \frac{C_s}{C_p} \times \frac{S_s}{K_p} \quad (7)$$

If the left-hand side of Eq. 7 is plotted against C_s/C_p for different binary mixtures, the slope of the regression line gives S_s/K_p, and the intercept S_p/K_p. For simplicity, $S_s = 1$ is generally adopted, whereby relative rather than absolute values of S_p are obtained. Under these conditions, Eq. 7 gives K_p and S_p at any wavelength.

The Kubelka–Munk theory has been successfully used to estimate the concentration of Fe oxides in soil samples (23, 24) and in kaolin for the paper industry (25). To this end, one must assign K and S values for the Fe oxides and for the matrix in which they are contained.

If we assume the scattering coefficient of Eq. 1 to vary little with wavelegth over the range of interest, the remission function and the actual absorption spectrum over such a wavelength range should be identical. This assumption was made for Fe oxides by Sherman and Waite (26).

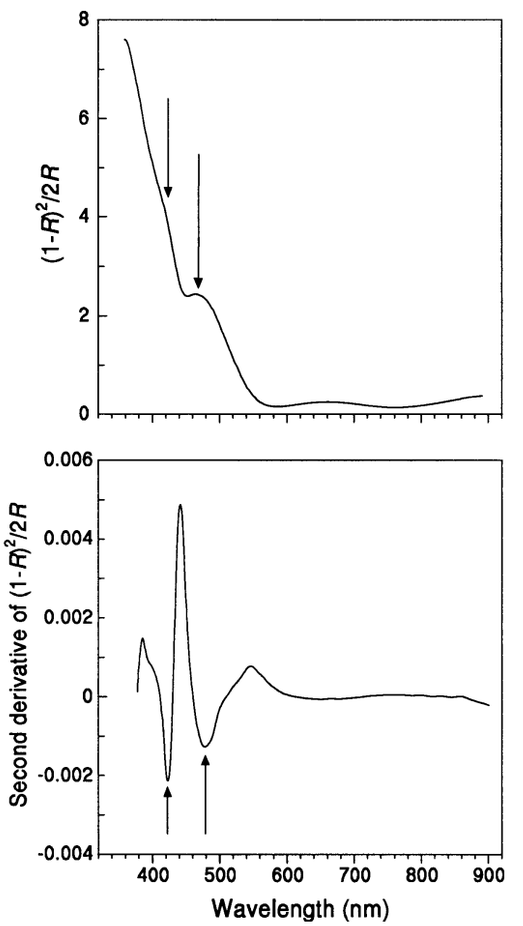

Fig. 4 The weak absorption bands in the remission function curve (*top*) become strong minima in the SD curve (*bottom*).

Derivative Spectroscopy

Diffuse reflectance spectra (or the corresponding remission function curves) result from the superposition of absorption bands at different wavelengths. Resolving the spectral curves into these bands is easier if the derivatives of the curves are previously obtained. The first derivative of a pure Gaussian absorption band has a maximum and a minimum to the left and right, respectively, of the maximum in the original band. The difference in ordinate between maximum and minimum is proportional to the band amplitude. The second-derivative (SD) curve has a minimum at the point of maximum curvature (peak) of the original absorption band. The SD curve usually provides more information than does the first-derivative curve because a band in the original spectrum, even when superimposed with other bands and not yielding a true absorption maximum (reflectance minimum), always yields a minimum in the SD curve. This key feature of SD curves is illustrated in Fig. 4 for a goethite sample.

Because spectra are obtained stepwise, they must generally be smoothed for calculation of their successive derivatives. Various algorithms are available for this purpose. The cubic spline fitting procedure (27) is based on joining a number of cubic polynomial segments end to end, based on a certain number of adjacent data points, with the restriction that continuity in the first and second derivative must exit in the joints. The method of Savitzky and Golay (28) is based on fitting a polynomial curve to a set of contiguous data points (usually from 13 to 31) by the least-squares method and calculating the ordinate at the central value of the abscissa (wavelength). A new polynomial curve is then obtained by moving the set one point and calculating the new ordinate. The derivative is obtained by calculating the slope at the central value of the abscissa. The number of points in each set is a crucial input parameter in both procedures. Goodness of fit increases, but degree of smoothing decreases (and resolution increases) with decreasing number of points, so a compromise must be adopted. Gálvez et al. (29) found 22 points to provide the best results when a cubic spline procedure was used for spectra obtained in 0.5-nm steps.

Absorption Bands: Significance, Identification, and Applications

The absorption bands exhibited by the Fe oxides at UV to near IR wavelengths originate from electronic transitions within the $3d^5$ shell of the Fe^{3+} ion. These transitions are as follows: 1) Fe^{3+} ligand field transitions, 2) transitions due to magnetically coupled Fe^{3+} cations in adjacent sites, and 3) the ligand-to-metal charge transfer (LMCT).

Fe $3d$ atomic orbitals are split into three t_{2g} and two e_g orbitals separated by an energy of $10Dq$ (the ligand field parameter or crystal field splitting). Ligand field (or d-d) transitions are ultimately due to the possible electronic configurations of these orbitals and are the result of excitations from the ${}^6A_1\ ({}^6S)$ ground state arising from the ground state $(t_{2g}^{\alpha})\ (e_g^{\alpha})$ configuration of high-spin Fe^{3+}. These transitions are in principle both spin and parity forbidden. However, they become allowed in Fe oxides through magnetic coupling of electronic spins of next-nearest-neighbor Fe^{3+} ions in the crystal. Additional transitions corresponding to simultaneous excitations within two adjacent Fe^{3+} ions may be present. These ''double-exciton'' processes result in bands in the visible region. Finally, LMCT transitions occur at energies higher than those of ligand field transitions and produce an absorption band in the near UV that extends onto the lower wavelengths (blue–green) of the visible region. This is responsible for the yellow to red hues of most Fe oxides.

The SD spectra of Fe oxides generally exhibit four bands in the visible to near IR region (380–1050 nm). In the light of the ligand field theory, Sherman and Waite (26) assigned three such bands to the following ligand field transitions: ${}^6A_1\ ({}^6S) \rightarrow {}^4T_1({}^4G), {}^6A_1\ ({}^6S) \rightarrow {}^4T_2({}^4G)$, and ${}^6A_1\ ({}^6S) \rightarrow {}^4E;{}^4A_1({}^4G)$. The fourth band was assigned to the electron pair transition or ${}^6A_1\ ({}^6S)$ double exciton

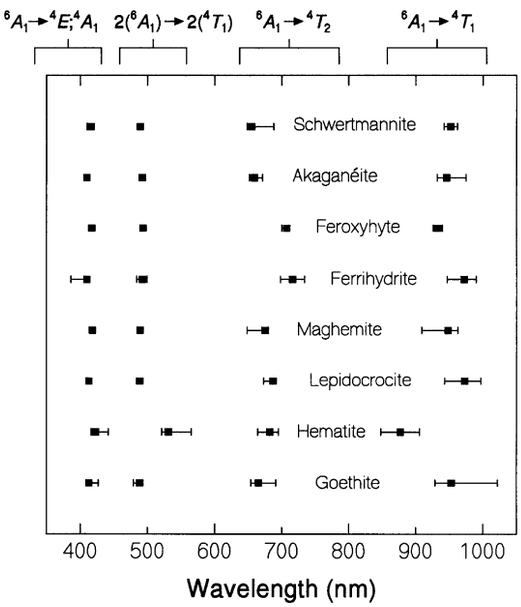

Fig. 5 Median and range of the position of the bands due to the most prominent electronic transitions of various Fe oxides. (Data taken from Ref. 30.)

$2\left({}^6A_1\right) \rightarrow 2\left[{}^4T_1({}^4G)\right]$. This double exciton process usually yields the strongest band, so it exerts a decisive influence on hue. Thus, goethite is yellow and hematite is red because the corresponding band lies at a lower wavelength in the former (~480 nm) than in the latter (~530 nm) (26).

Scheinost et al. (30) used SD spectroscopy to examine the intensity of these four bands for 176 synthetic and natural Fe oxide samples. They found significant differences in band position and intensity among the eight minerals studied and also among different samples of each mineral. These differences arise in the first place because $Fe(O, OH)_6$ octahedra are linked in different ways, as shown by x-ray absorption spectroscopy (31). Distortion of the octahedra results in decreased symmetry and in consequent change in ligand field and band position (5). Also, differences in the Fe-to-Fe distance and in the degree of occupancy of octahedra are likely to affect magnetic coupling of the neighbor Fe^{3+} ion and, as a result, the position and intensity of the double exciton band. The combined effect of all these factors results in substantial overlap of the bands for different oxides, as shown in Fig. 5. So, Scheinost et al. (30) found that: 1) pure samples of goethite, maghemite, and schwertmannite could not be discriminated; 2) at least 80% of pure akagenéite, feroxyhyte, ferrihydrite, hematite, and lepidocrocite samples were correctly classed by using discriminant functions; and 3) in soil mixtures containing other Fe oxides, only hematite and magnetite could be discriminated from other Fe oxides. In summary, band overlap generally constitutes a hindrance to Fe oxide identification by DR. For instance, this problem, together with poor spectral resolution, has precluded positive identification of Fe oxides in Martian soils and dust. Such a presence is suggested by the ~870-nm band in the ''bright-region'' spectra, which can be assigned to the ${}^6A_1 \rightarrow {}^4T_1$ transition (5, 32–34).

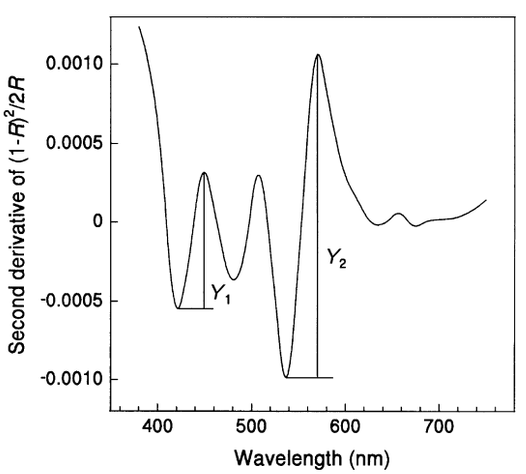

Fig. 6 Position and amplitude of the bands selected for quantification of goethite (Y_1) and hematite (Y_2) in soils. (From Ref. 30.)

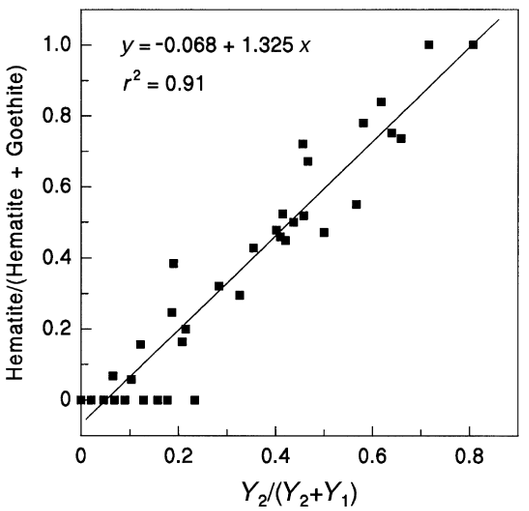

Fig. 7 Relationship between the hematite/(hematite + goethite) ratio as determined by differential x-ray diffraction and the $Y_2/(Y_1 + Y_2)$ ratio, as determined by diffuse reflectance spectroscopy. (From Ref. 30.)

Several studies have suggested that DR spectra may shed light on the crystal properties of Fe oxides. Thus, the ${}^6A_1 \rightarrow {}^4T_1$ transition of goethite was shifted to lower energy (longer wavelength) by incorporation of Al into the structure. Buckingham and Sommer (35) attributed this to the decrease in unit-cell length toward that of diaspore (α-AlOOH, isomorphous with goethite), with a concomitant decrease in Fe–(O, OH) distances and an increase in $10Dq$. Similar results were obtained for hematite (36). Scheinost et al. (10) investigated the DR spectra of Al-substituted goethite $\left[\alpha\text{-}Fe_{(1-x)}Al_xOOH\right.$, with x ranging from 0 to 0.33$\left.\right]$ by fitting four electron transitions as a function of $10Dq$ and the interelectronic repulsion parameters Racah B and C. From changes in $10Dq$, they estimated a decrease in the Fe–(O, OH) distance from 202.0 to 200.9 pm as x was increased from 0 to 0.33. Such a decrease was smaller than that in the Fe–(O, OH) distance calculated from the change in unit-cell length, the divergence being attributed to the presence of diaspore clusters within the Al-substituted goethite crystals.

Gálvez et al. (29) used DR spectroscopy to study the crystal properties of hematite prepared by hydrolysis of $Fe(NO_3)_3$ in the presence of phosphate. The hematites incorporated P in an occluded, nondesorbable form, and exhibited an absorption band at ~488 nm that could not be

ascribed to any reported transition for hematite (26). It did, however, coincide with the $2\left({}^6A_1\right) \rightarrow >2\left[{}^4T_1\left({}^4G\right)\right]$ exciton for goethite. Increasing the P content in hematite increased the ratio of the SD amplitude of this band to that of the homonymous band for hematite (~538 nm). This was interpreted as an increased ''goethitic'' character in the hematite, which was attributed to the presence of structural P in tetrahedral sites (and the consequent Fe deficiency in the cationic substructure), as well as to an increase in structural OH content.

Detection limits in SD spectroscopy are smaller than in other identification techniques for Fe oxide bands. Thus, less that 0.1% goethite and hematite can be detected in mixtures with other soil minerals (30); this percentage is more than one order of magnitude smaller than the detection limit of ordinary x-ray diffraction. This advantage is also provided by first-derivative spectroscopy (37). It should be noted, however, that the intensity of any specific band in the SD curve is in practice roughly proportional to the concentration of the corresponding Fe oxide only at concentrations usually below 5% (30). This, together with the large differences in band intensity exhibited by different samples of the same Fe oxide, hinder quantification of individual Fe oxides in a mixture.

Because of matrix effects in quantitative analyses, it is advisable to estimate relative rather than absolute amounts of Fe oxides in mineral mixtures (provided that oxides have characteristic and, mainly, nonoverlapping bands). For instance, many soils and sediments contain significant amounts of goethite and hematite as the only Fe oxides. Based on this, Scheinost et al. (30) used the intensity of the SD band between the ~415-nm minimum $\left({}^6A_1 \rightarrow {}^4A_1; {}^4E\right)$ and the 445-nm maximum for goethite (denoted as Y_1), and that between the ~535-nm minimum (double exciton) and the 580-nm maximum for hematite (denoted as Y_2) (Fig. 6), to estimate the hematite–goethite ratio. For a population of 40 soils ranging widely in properties, significant correlation was thus found between the hematite / (hematite + goethite) ratio and the $Y_2 / (Y_1 + Y_2)$ ratio (Fig. 7).

CONCLUSION

Diffuse reflectance spectroscopy is applicable to fine-size materials consisting of or containing Fe oxides. Diffuse reflectance spectra can be readily and conveniently acquired with modern spectrophotometers, and provide a rigorous method for describing the color of a powder. Parameterization of these spectra in various ways is useful with a view to identifying individual Fe oxides in a mixture, the ensuing detection limits being much lower than in other techniques such as x-ray diffraction. Discriminating between some Fe oxides, however, is not always possible. Fine analysis of the absorption bands based on SD curves of the original reflectance spectrum or the remission function has been successfully used to: 1) identify and quantify Fe oxides in a mixture, and 2) infer the crystal properties of some Fe oxides. Exploitation of the potential of diffuse reflectance spectroscopy is still in its infancy. This, together with its simplicity, make this technique an interesting alternative or complement to others used in the study of Fe oxides.

ACKNOWLEDGMENTS

This work was supported by Spain's CICYT under Project PB98–1015.

REFERENCES

1. Scheinost, A.C.; Schwertmann, U. Color identification of iron oxides and hydroxysulfates: use and limitations. Soil Sci. Soc. Am. J. **1999**, *63* (5), 1463–1471.
2. Kortüm, G. Regular and Diffuse Reflection. In *Reflectance Spectroscopy*; Springer-Verlag: Berlin, 1969; 5–71.
3. Hunter, R.S. Attributes of the Appearance of Objects. In *The Measurement of Appearance*; John Wiley & Sons: New York, 1975; 3–17.
4. Torrent, J.; Barrón, V. Laboratory Measurement of Soil Color: Theory and Practice. In *Soil Color*; Bigham, J.M., Ciolkosz, E.J., Eds.; SSSA Special Publication No. 31, Soil Science Society of America: Madison, 1993; 21–33.
5. Burns, R.G. Remote-Sensing Composition of Planetary Surfaces: Applications of Reflectance Spectra. In *Mineralogical Applications of Crystal Field Theory,* 2nd Ed.; Cambridge Topics in Mineral Physics and Chemistry No. 5, Cambridge University Press: Cambridge, United Kingdom, 1993; 396–427.
6. Torrent, J.; Schwertmann, U. Influence of hematite on the color of red beds. J. Sediment. Petrol. **1987**, *57* (4), 682–686.
7. Wyszecki, G.; Stiles, W.S. Colorimetry. In *Color Science: Concepts and Methods, Quantitative Data and Formulae,* 2nd Ed.; John Wiley & Sons: New York, 1982; 117–248.
8. CIE (Commission Internationale de L'Eclairage). *Recommendations on Uniform Color Spaces, Color-Difference Equations, Psychometric Color Terms. Supplement no. 2 to Publ. no. 15, Colorimetry*; Bureau Central de la CIE: Paris, 1978; 1–21.
9. Schwertmann, U. Relations Between Iron Oxides, Soil Color, and Soil Formation. In *Soil Color*; Bigham, J.M., Ciolkosz, E.J., Eds.; SSSA Special Publication No. 31, Soil Science Society of America: Madison, 1993; 51–69.
10. Scheinost, A.C.; Schulze, D.G.; Schwertmann, U. Diffuse

reflectance spectra of Al substituted goethite: a ligand field approach. Clays Clay Miner. **1999**, *47* (2), 156–164.
11. Barrón, V.; Torrent, J. Influence of aluminum substitution on the color of synthetic hematites. Clays Clay Miner. **1984**, *32* (2), 157–158.
12. Kosmas, C.S.; Franzmeier, D.P.; Schulze, D.G. Relationships among derivative spectroscopy, color, crystallite dimensions, and Al substitution of synthetic goethites and hematites. Clays Clay Miner. **1986**, *34* (6), 625–634.
13. Stiers, W.; Schwertmann, U. Evidence for manganese substitution in synthetic goethite. Geochim. Cosmochim. Acta **1985**, *49*, 1909–1911.
14. Torrent, J.; Schwertmann, U.; Schulze, D.G. Iron oxide mineralogy of some soils of two river terrace sequences in Spain. Geoderma **1980**, *23* (2), 191–208.
15. Schwertmann, U.; Murad, E.; Schulze, D.G. Is there holocene reddening (hematite formation) in soils of axeric temperate areas? Geoderma **1982**, *27* (2), 209–223.
16. Torrent, J.; Schwertmann, U.; Fechter, H.; Alférez, F. Quantitative relationships between color and hematite content. Soil Sci. **1983**, *136* (6), 354–358.
17. Kemp, R.A. The cause of redness in some buried and non-buried soils of eastern England. J. Soil Sci. **1985**, *36* (3), 329–334.
18. Torrent, J.; Cabedo, A. Sources of iron oxides in reddish brown soil profiles from calcarenites in southern Spain. Geoderma **1986**, *37* (1), 57–66.
19. Boero, V.; Schwertmann, U. Occurrence and transformation of iron and manganese in a colluvial terra rossa toposequence in northern Italy. Catena **1987**, *14* (6), 519–531.
20. Kubelka, P.; Munk, F. Ein Beitrag zur Optik der Farbanstriche. Z. Tech. Phys. **1931**, *12*, 593–620.
21. Kortüm, G. Phenomenological Theories of Absorption and Scattering of Tightly Packed Particles. In *Reflectance Spectroscopy*; Springer-Verlag: Berlin, 1969; 103–169.
22. Duncan, D.R. The colour of pigment mixtures. Proc. Phys. Soc. **1940**, *52*, 390–401.
23. Barrón, V.; Torrent, J. Use of the Kubelka-Munk theory to study the influence of iron oxides on soil colour. J. Soil Sci. **1986**, *37* (4), 499–510.
24. Fernandez, R.N.; Schulze, D.G. Munsell colors of soils simulated by mixtures of goethite and hematite with kaolinite. Z. Pflanzenernaehr. Bodenkd. **1992**, *155* (5/6), 473–478.
25. Jepson, W.B. Structural Iron in Kaolinites and in Associated Ancillary Minerals. In *Iron in Soils and Clay Minerals*; Stucki, J.W., Goodman, B.A., Schwertmann, Eds.; NATO ASI Series, Series C: Mathematical and Physical Sciences, Vol. 217, Reidel Publ. Co.: Dordrecht, The Netherlands, 1988; 467–536.
26. Sherman, D.M.; Waite, T.D. Electronic spectra of Fe^{3+} oxides and oxide hydroxides in the near IR to near UV. Am. Mineral. **1985**, *70*, 1262–1269.
27. Press, W.H.; Teukolsky, S.A.; Vetterling, W.T.; Flannery, B.P. Interpolation and Extrapolation. In *Numerical Recipes in Fortran,* 2nd Ed.; Cambridge University Press: Cambridge, United Kingdom, 1992; 99–122.
28. Savitzky, A.; Golay, M.J.E. Smoothing and differentiation of data by simplified least squares procedures. Anal. Chem. **1964**, *36* (8), 1627–1640.
29. Gálvez, N.; Barrón, J.; Torrent, J. Preparation and properties of hematite with structural phosphorus. Clays Clay Miner. **1999**, *47* (3), 375–385.
30. Scheinost, A.C.; Chavernas, A.; Barrón, V.; Torrent, J. Use and limitations of second-derivative diffuse reflectance spectroscopy in the visible to near-infrared range to identify and quantify Fe oxides in soils. Clays Clay Miner. **1998**, *46* (5), 528–536.
31. Manceau, A.; Combes, J.M. Structure of Mn and Fe oxides and oxyhydroxides: a topological approach by EXAFS. Phys. Chem. Miner. **1988**, *15*, 283–295.
32. Bishop, J.L.; Murad, E. Schwertmannite on Mars? Spectroscopic Analyses of Schwertmannite, Its Relationship to Other Ferric Minerals, and its Possible Presence in the Surface Material of Mars. In *Mineral Spectroscopy: A Tribute to Roger G. Burns*; Dyar, M.D., McCammon, C., Schaefer, M.W., Eds.; Special Publication No. 5, The Geochemical Society: St. Louis, Missouri, 1996; 337–358.
33. Morris, R.V.; Golden, D.; Bell, J.F.I. Low-temperature reflectivity spectra of red hematite and the color of Mars. J. Geophys. Res. **1997**, *102* (E4), 9125–9133.
34. Bell, J.F.I.; MsSween, H.Y.J.; Crisp, J.A.; Morris, R.V.; Murchie, S.L.; Bridges, N.T.; Johnson, J.R.; Britt, D.T.; Golombek, M.P.; Moore, H.J.; Ghosh, A.; Bishop, J.L.; Anderson, R.C.; Brückner, J.; Economou, T.; Greenwood, J.P.; Gunnlaugsson, H.P.; Hargraves, R.M.; Hviid, S.; Knudsen, J.M.; Madsen, M.B.; Reid, R.; Rieder, R.; Soderblom, L. Mineralogical and compositional properties of Martian soil and dust: results from Mars Pathfinder. J. Geophys. Res. **2000**, *105* (E1), 1721–1755.
35. Buckingham, W.F.; Sommer, S.E. Mineralogical characterization of rock surfaces formed by hydrothermal alteration and weathering-application to remote sensing. Econ. Geol. **1983**, *78*, 664–674.
36. Morris, R.V.; Schulze, D.G.; Lauer, H.V.; Agresti, D.G.; Shelfer, T.D. Reflectivity (visible and near IR), Mössbauer, static magnetic, and X-ray diffraction properties of Al-substituted hematites. J. Geophys. Res. **1992**, *97* (E6), 10257–10266.
37. Deaton, B.C.; Balsam, W.L. Visible spectroscopy-a rapid method for determining hematite and goethite concentration in geological materials. J. Sediment. Petrol. **1991**, *61*, 628–632.